The Electrochemical Society
Advancing solid state & electrochemical science & technology

Effective Particle Analysis on Wafer in the EKF-CMP System

View the article online for updates and enhancements.

Effective Particle Analysis on Wafer in the EKF-CMP System

Phuoc-Trai Mai,[1] Li-Shin Lu,[2] Chao-Chang A. Chen,[1,z] and and Yu-Ming Lin[1]

[1]*Department of Mechanical Engineering, National Taiwan University of Science and Technology, Taiwan*
[2]*Department of Industrial Engineering and Management, National Quemoy University, Kinmen, Taiwan*

This study aims to develop a three-dimensional electro-osmosis flow (3D-EOF) cell model for effective particle analysis on the wafer at steady-state under electro-kinetic force (EKF) assistance during chemical mechanical polishing/planarization (CMP). A simulation software is used to simulate the abrasive particle motion with three functional modules including the electric current, the laminar flow, and the particle trajectories. Parameter designs of various simulation conditions such as electrode gap spacing, direct current voltages, and polishing pad thickness have been investigated to analyze the motion of silica abrasive nanoparticles due to EOF. Simulation results of the EOF velocity of slurry flow circulation in different conditions have compared with theoretical calculation results. Results have shown that the total number of effective particles intensifies significantly with increasing electrode voltage, but decreases in both cases as raising electrode gap and larger pad thickness. Experimental results of EKF-CMP process can improve 25.03%, 2.52 nm, 1.39% for material removal rate (MRR), surface roughness, non-uniformity, respectively. It can explain that the wafer surface polishing qualification is significantly by motion of effectual abrasive particles. Results of this study can be extended to contribute to improvement and optimization of EKF-CMP process for Copper CMP process used in IC fabrication.

Slurry has an important role in the material removal rate (MRR) of chemical mechanical polishing/planarization(CMP) process which has been a popular wafer and thin-film planarization process in semiconductor fabrication.[1,2] It is a material removal process to polish flat surfaces on silicon substrates or partially-processed wafers during the semiconductor manufacturing industry for production of integrated circuit (IC) devices.[2,3] In CMP process, the pad is placed on a rotating platen, the wafer is held by a rotating carrier, the wafer surface is pressed against the pad surface, the slurry flow includes high purity water, chemical solution, and abrasive particles which are injected on the pad surface and then immersed into the gap between wafer and pad. The gap between wafer and pad depends on the loading pressure applied on the carrier.[4,5]

To calculate the MRR in the CMP process, the following Preston empirical equation is used to describe the CMP performance of MRR for a long period of time[6–10]

$$MRR = KPV \qquad [1]$$

In Eq. 1, where K is Preston's constant which depends on the chemical and mechanical aspects, P is downforce, and V is linear velocity ratio which depends on the product of the platen rotation speed and the distance between the platen center and the wafer center. Material is removed from the wafer surface due to the chemical action of the slurry flow velocity, the mechanical action of the abrasive particles on the polishing pad, and the relative velocity ratio between the rotating pad and the rotating wafer.[11,12] The relative velocity affects directly the slurry flow velocity from the inlet spread on the pad surface and entered the pad-slurry-wafer interactions.[13] Therefore, one of the most fundamental factors in the CMP process is considered as the slurry flow velocity.[14,15] The slurry flow has many properties including slurry flow rate, fluid pressure, the viscosity and density of the slurry, abrasive particle concentration (wt%), abrasive particle size, particle deformation, chemical additives, pH value, and temperature.[16] Almost all these parameters have influence on wafer surface quality.

From above survey , researchers have developed a lot of slurry flow models in CMP to observe the behavior of slurry flow distribution in the pad-slurry-wafer interactions.[17–19] The wafer and pad surfaces are separated by a slurry thin film. This slurry layer supports totally the loading pressure applied on the carrier and determines material removal on the wafer surface.[20] The minimum slurry film thickness was examined in a three-dimensional chemical mechanical planarization slurry flow model based upon lubrication theory by Thakurta et al.[21] Additionally, modeling and simulation for abrasive particle behavior and slurry distribution in the interface have been developed by Nguyen et al. In this article, the distribution of abrasive particles in the slurry between the wafer and pad surfaces have been investigated using a multiphase 3D computational fluid dynamics model.[22] A hydrodynamic and kinematic analysis and a new geometrical model of the formation of the machined surface have been reviewed by Qi and Mai et al.[23,24] Chen et al. mentioned the finite-element analysis on wafer-level CMP contact stress under the effects of selected process parameters.[25] There were other formulas from other researchers to analyze the relationship between polish rate uniformity and lubrication theory based on a three-dimensional hydrodynamic flow model.[26] Moreover, several researchers focused on experimental and numerical analysis using digital image processing which was also contributed to slurry flow fields in the CMP process.[27,28] Additionally, the slurry is a key material to use its silica abrasive nanoparticle to cut the passivation layer of the wafer surface. The random or distributed motions of the particles in the slurry will affect MRR and wafer surface roughness. To improve the local slurry circulation, we have developed the technique of electro-kinetic force assisted for the CMP process by the applied electro-osmotic flow, it is called the EKF-CMP system.[29,30] The EKF-CMP system can improve the MRR with 22.29% for Cu-Blanket film and 9.52% for glass wafer. To quantify the fluctuation motions of abrasive particle in slurry, this study defines the effective particles as the total number of abrasive particle motion to contact with the wafer surface in the EKF-CMP system. The behavior of effective particle motion is very important in CMP. However, the effective particle motion on the wafer surface at steady-state with various conditions of conductive platen design in the EKF-CMP system has not yet fully analyzed.

To investigate the optimal conductive platen design for the electrode gap spacing and polishing pad thickness in the EKF-CMP system, this research develops a 3D-EOF cell model to simulate and analyze the total number of effective particles on the wafer for the dynamic behavior of silica abrasive nanoparticle inside the slurry film thickness due to the energy of EKF. The 3D-EOF cell model structure is built in COMSOL Multiphysics® software with the applied three functional modules including electric current,

zE-mail: artchen@mail.ntust.edu.tw

laminar flow, and particle trajectories. The relationship between the total number of effectual particles at steady-state and the various parameters such as the electrode gap spacing, the direct current voltages, the polishing pad thickness is investigated to explore the important role of the different variables affecting the abrasive particle's motion and then for MRR in EKF-CMP system. Results of this research can contribute to the improvement and development of EKF-CMP technology for IC fabrication process.

Fundamental Theory

Electro-kinetic force (EKF).—Electro-kinetic transport phenomena are mainly used to explain fluid mechanics, colloidal phenomena, the interaction between solid surfaces and electrolytes under the conditions of an applied external electric field.[31] The EKF principle has a long history in colloid science, which defines heterogeneous fluids with charged particles in the size of micrometers or nanometers in an environment where an electric field generates Coulomb force, as follow[32]

$$F = qE_t \qquad [2]$$

where F is the electric field force, q is the magnitudes of the charge density, and E_t is the electric field strength. The EKF assists the particle-liquid interface with an electric double layer. The force generated by the externally applied electric field drives the fluid disturbance phenomenon. The EKF function provides the electric actuation in the CMP process, intermediates electro-osmosis flow which increases the grinding disturbance of the particle-free fluid, and increases the number of effective particles on the polishing pad surface. Fig. 1 shows the simple model of EKF-CMP system of the electro-osmosis flow (EOF) in the slurry film thickness of the polishing pad without the groove and pad porosity.

Electric double layer (EDL).—Electric double layer (EDL) is mainly produced at the particle-liquid interface. By attracting counter-ions in electrically neutral liquids and promoting the concentration of liquid hetero-ions close to the solid surface area to be higher than that of co-ions. The ions can accumulate into a charge layer on the electrode surface called the EDL. Most of the particle-liquid interfaces have charges. As shown in Fig. 2, the electric double-layer model was first proposed by Helmholtz in 1853.[33] It assumed that the positive and negative ions correspond to each other in a one-to-one ratio to form an electric double layer. The layers were composed like a parallel plate capacitor model. One layer was the surface charge through the solid, another layer was the

ion center plane in the solution that was electrostatically attracted to the metal surface, and the ion radius was regarded as the thickness of the electric double layer. According to the charged ion radius of different elements, it could be judged that the thickness range was about 0.02 to 20 nm, but the model proposed by Helmholtz only considered the mutual attraction caused by the electrostatic force and ignored the thermal motion of the molecule. It could not explain the electric double layer. The correlation between the layer capacitance value, the electrode potential, and the electrolyte concentration was later proposed by Gouy and Chapman et al. In 1910 to 1913.[33] The theory of dispersed electric double layer was revised, and the corresponding ion in the solution was gradually diffused. They believed that the flat electric double layer model proposed by Helmholtz was not the same as the actual result. The counterions in the solution were not bound in parallel in the liquid phase adjacent to the particle surface, but were diffusely distributed in the space around the particles. Their concentration decreased with the increasing distance from the particle. Finally, in 1924, Stern proposed an electric double-layer model integrating Helmholtz and Gouy-Chapman.[34] This model divided the electric double layer into two layers due to the high and low concentration of the anisotropic ion. It was attracted by the opposite ions of the charged solid interface, so the closer the interface was, the higher the charged ion concentration was formed a charge layer different from the solid surface charge. This layer was defined as a fixed layer, and the farther away from the fixed layer was the surface. The binding force of the ions given by the potential was weak, and the concentration decreases with the increasing distance, which was called a diffuse double layer.[35]

Starting from the surface potential φ_0, the potential will decrease linearly until the interface potential φ_d of the fixed layer and the diffusion layer, also known as the zeta potential (ζ). When the distance increases to the diffusion layer, the potential will begin to show a decreasing trend. The relationship that the characteristic distance of Countdown is the electric double layer thickness degree $\varphi = \varphi_0 e^{-kr}$, which is called Debye Length degree (K^{-1}). The relationship defining the electric double layer thickness degree can be obtained from Eq. 3:

$$K^{-1} = \left(\frac{\varepsilon k_B T}{2Z^2 q^2 n_0} \right)^{0.5} \qquad [3]$$

Where ε is the dielectric constant, k_B is the Boltzmann constant, T is the absolute temperature, z is the number of ionic charges, q is the
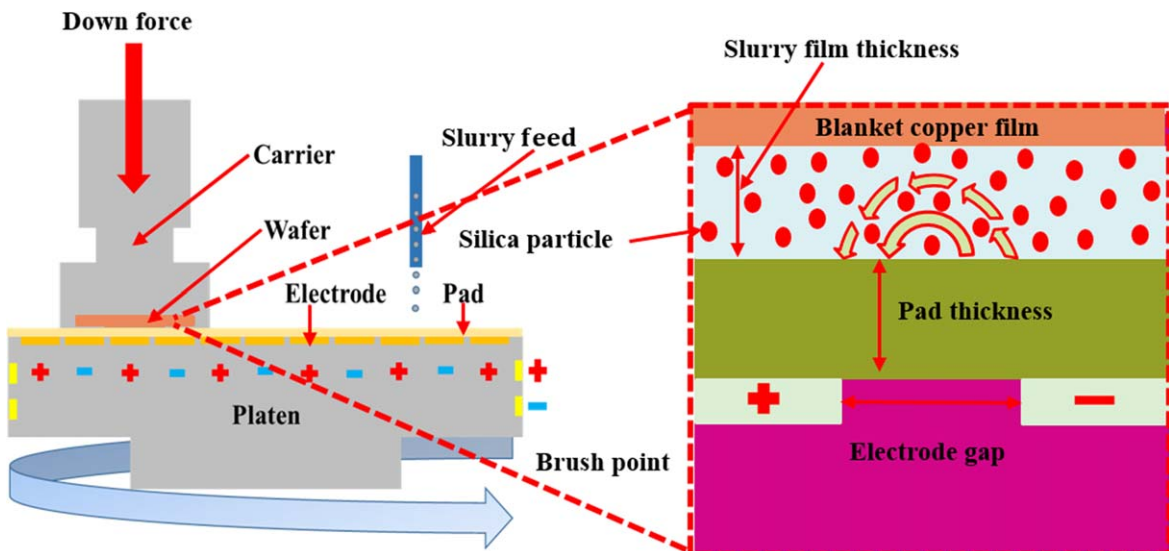

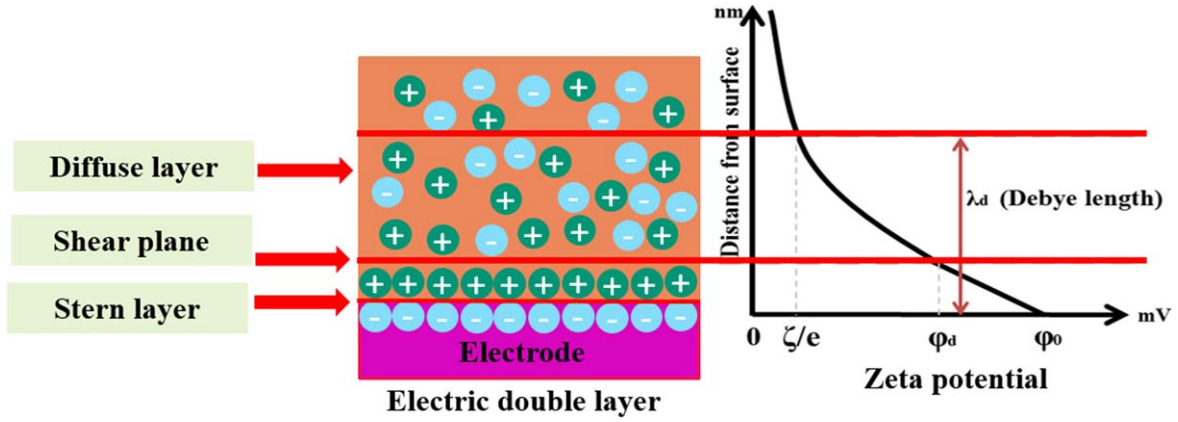**Figure 1.** Schematic diagram of electro-osmosis flow in EKF-CMP.

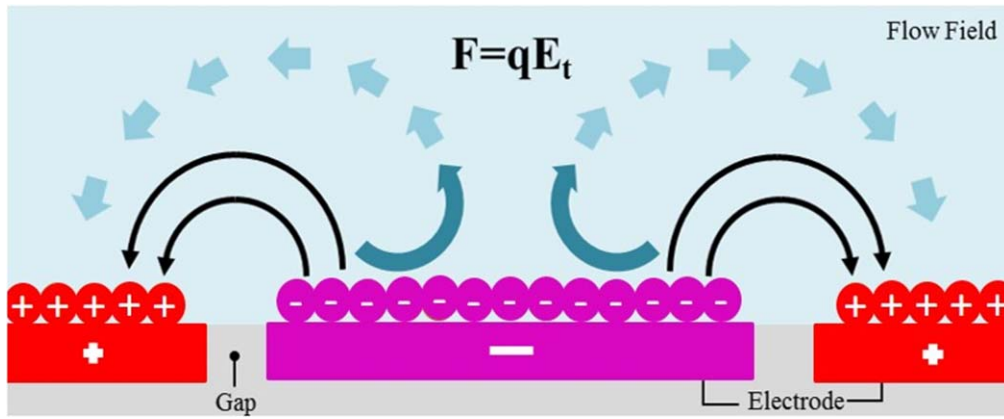**Figure 2.** Schematic diagram of electric double layer composition.

Figure 3. Schematic diagram of electro-osmosis flow disturbance.

number of electron charges, n_0 is the ion concentration. The potential between the diffusion layer and the fixed layer in the electric double layer is called the boundary potential (ζ). According to Debye-Huckel's theory, the interface in the solution will absorb opposite charges to form an electric double layer due to the accumulation of surface charges. Due to the shadowing phenomenon, its potential will decay exponentially, causing its potential to exhibit exponential decay. In an environment where the general fluid is water, its potential is:

$$\zeta = \frac{-\sigma_d}{\varepsilon K} \qquad [4]$$

It can be seen from Eq. 4 that the thickness of the electric double layer is directly proportional to the Zeta potential, where σ_d is the surface charge density.

Electric osmosis flow (EOF).—The electro-osmosis flow (EOF) phenomenon is that the presence in the solution causes the particle-liquid interface to form an electric double layer, which generates an electric actuation force that changes the abortion due to the electric field effect, as shown in Fig. 3. At this time, suppose that an electric field in the direction of the line acts on the electric double layer of the charged surface such as the electrode, which will produce an effect force. The potential of the diffusion layer in the electro-electric double-layer moves, so that the entire flow is dragged flow. This dynamic phenomenon is called electro-osmosis flow. EOF phenomena can occur in both direct current (DC) and alternating current (AC) electric fields.[34,35] At present, most researches on the EOF are micro-channel pumps and cell collection of biochips. This

study will focus on electro-osmosis phenomena in direct current electric fields. According to Coulomb's law the velocity of the EOF is proportional to the magnitude of the tangential electric field and the electric force acting on the particle-free liquid. The velocity of the EOF is calculated as Eq. 6 for a plane flow microchannel, and the EOF velocity is obtained by the electro-osmosis mobility as follows

$$\mu = \frac{u_{eof}}{E_t} = -\frac{\varepsilon\zeta}{\eta} = -\frac{\varepsilon_r \varepsilon_0 \zeta}{\eta} \qquad [5]$$

$$u_{eof} = \mu \times E_t \qquad [6]$$

where μ is the electro-osmosis mobility, u_{eof} is the electro-osmosis flow velocity, E_t is the applied electric field intensity, ζ is the zeta potential, ε is the liquid permittivity, η is the dynamic viscosity of the liquid, ε_r is the relative permittivity, ε_0 is the free space permittivity. This rate has a direct relationship with the electric field size and the charge density of zeta potential in the electric double layer in the EOF velocity, so it can be rewritten as follow

$$u_{eof} = \frac{E_t \sigma_d}{\eta K} \qquad [7]$$

where σ_d is the surface charge density, K is Debye length degree.

The electro-osmosis force is applied to the chemical mechanical planarization process, the positive and negative electrodes are embedded in the conductive disk, and the polishing pad with non-
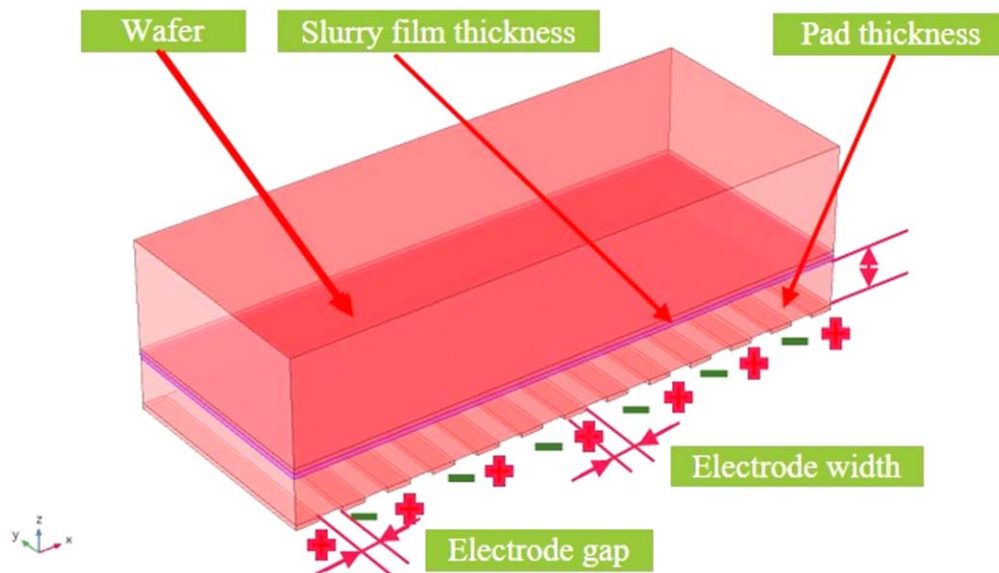
Figure 4. Simulation structure of the three-dimensional of the electro-osmosis flow cell model in EKF-CMP.

Table I. Simulation parameter for 3D-EOF cell model.

Parameters	Value (Unit)
Pad material	Polyurethane (Solid PU)
Pad stiffness	5 Mpa
Wafer material	Copper film
Wafer hardness	1.75 Gpa
Wafer thickness	0.1 mm
Wafer length	12 mm
Wafer width	4 mm
Slurry type	DI-Water
Slurry film thickness	50 μm
Slurry density	1000 kg/m^3
Slurry dynamic viscosity	0.001 kg/m−s
Slurry PH	3.5
Slurry pressure	1 Pa
Particle type	Silica (SiO$_2$)
Particle density	2650 kg/m^3
Particle dynamic viscosity	0.005 Pa.s
Particle diameter	20 nm
Particle number	5000
Particle bulk hardness	2.0 GPa
Particle concentration	0.03%
Sink length	12 mm
Sink width	4 mm
Sink height	4 mm
Pad thickness	1 mm, 1.2 mm, 1.4 mm, 1.6 mm, 1.8 mm 2 mm
Electrode material	Solid copper
Electrode width	1 mm
Electrode gap	1 mm, 1.5 mm, 2 mm, 2.5 mm, 3 mm
DC voltage application	10V, 30V, 50V, 70V, 90V
Zeta potential	−0.1 V
Relative permittivity	80
Particle tracing simulation time	500 s

grooves is pasted on the conductive disk. When a voltage is applied between the positive and negative electrodes on the polishing pad, electro-osmosis force can occur, which will disturb polishing liquid. This action can improve the efficiency of polishing liquid. The CMP process will effectively improve the planarization efficiency and reduce the defects.

Simulation Model Development of the 3D-EOF Cell Model

3D-EOF cell model in COMSOL.—Based on the computation fluid dynamic (CFD) simulation method of the particle element in the COMSOL Multiphysics® simulation software,[36] this study focuses on the analysis of a new generation of the EOF module approaching the actual EKF-CMP process and the observation of the
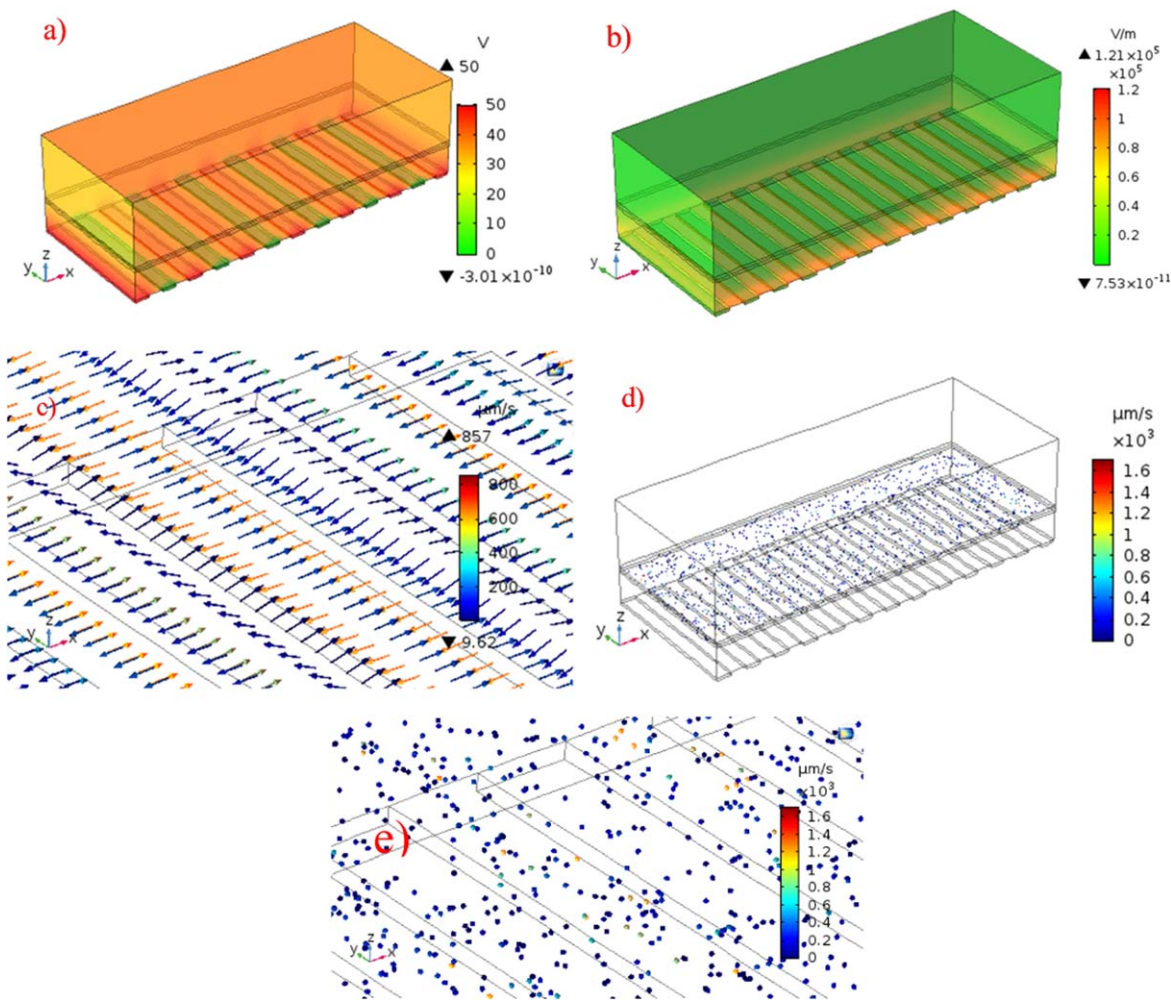
Figure 5. Simulation results of the electro-osmosis flow cell in EKF-CMP process at the electro gap of 1 mm, the pad thickness of 2 mm, and the applied voltage of 50V. (a) Electric potential, (b) Maximum tangential electric field, (c) Flow velocity, (d) Particle tracing, (e) Zoom in of particle tracing.

abrasive particle motion. The purpose of simulation is to observe the EOF strength by changing the electrode gap spacing and the polishing pad thickness to investigate the number of effective particles on wafer at steady-state to find a suitable conductive platen design for the EKF-CMP system.

The simulation structure of three-dimensional electro-osmosis flow cell model is mainly divided into four layers. The geometry of the components is shown in detail in Fig. 4, and the dimension of the 3D-EOF cell model is described in Table I. The first bottom layer mainly simulates the interleaved electrodes on the conductive disk. The electrode material is defined as solid copper with a minimum electrode width of 1 mm due to manufacturing process limitations. The form of a staggered arrangement of positive and negative electrodes is shown in Fig. 4. The specification of the electrode gap spacing is selected from 1 to 3 mm with raising step of 0.5 mm of five total sets of variation parameters. The DC voltage parameters are applied 10V, 30V, 50V, 70V, and 90V, respectively. The second layer is simulated as a polishing pad. The pad stiffness is 5 MPa with non-grooved and non-asperity. The material is polyurethane (PU) that most commercial polishing pads used as IC-1000 or SUBA 600. The thickness of polishing pad refers to thickness range of polishing pad most commonly used in our previous studies. Therefore, it is assumed that the thickness increases from 1 to 2 mm with raising step of 0.2 mm. The polishing pad thickness is built without the groove geometry and the pad porosity in the simulation model. The third layer is

simulated the slurry film thickness. The liquid layer is defined as deionization water (DI-Water). The consideration of liquid level comes from the definition of effective working areas on the polishing pad surface which is mainly divided into three regions. The upper area of pad asperity deformation of pad surface is the reaction region. The intermediate area calls the transition region, which provides the space for the flow of polishing liquid or slurry to activate the wafer reaction. The lower area is the reservoir region, which is used to provide the storage region for polishing liquid. When the polishing pad surface is deformed under the pressure, the polishing liquid is transferred from the storage region to the transfer area to reach the wafer. The average gap between the smooth wafer and the pad surface is about 20 μm and 100 μm. Therefore, the liquid level of the 3D-EOF cell model is set to be 50 μm, the liquid density is 1000 kg/m^3, the liquid dynamic viscosity is 0.001 kg/m−s, the particle type is silica, the particle diameter is 20 nm, the particle density is 2650 kg/m^3, the particle dynamic viscosity is 0.005 Pa.s, the bulk hardness is 2.0 GPa, the number of particles is 5000 which depends on the particle concentration of 0.3 wt% in the slurry film thickness. The fourth layer is the wafer. The wafer material is solid copper. The wafer hardness is 1.75 GPa without surface roughness. The wafer thickness is 0.1 mm. The wafer length is 12 mm. The wafer width is 4 mm. The original wafer size is referred to Semiconductor Materials Briefs (SEMI). In the COMSOL Multiphysics® software, the mesh element value must be lower than 0.95. The mesh model
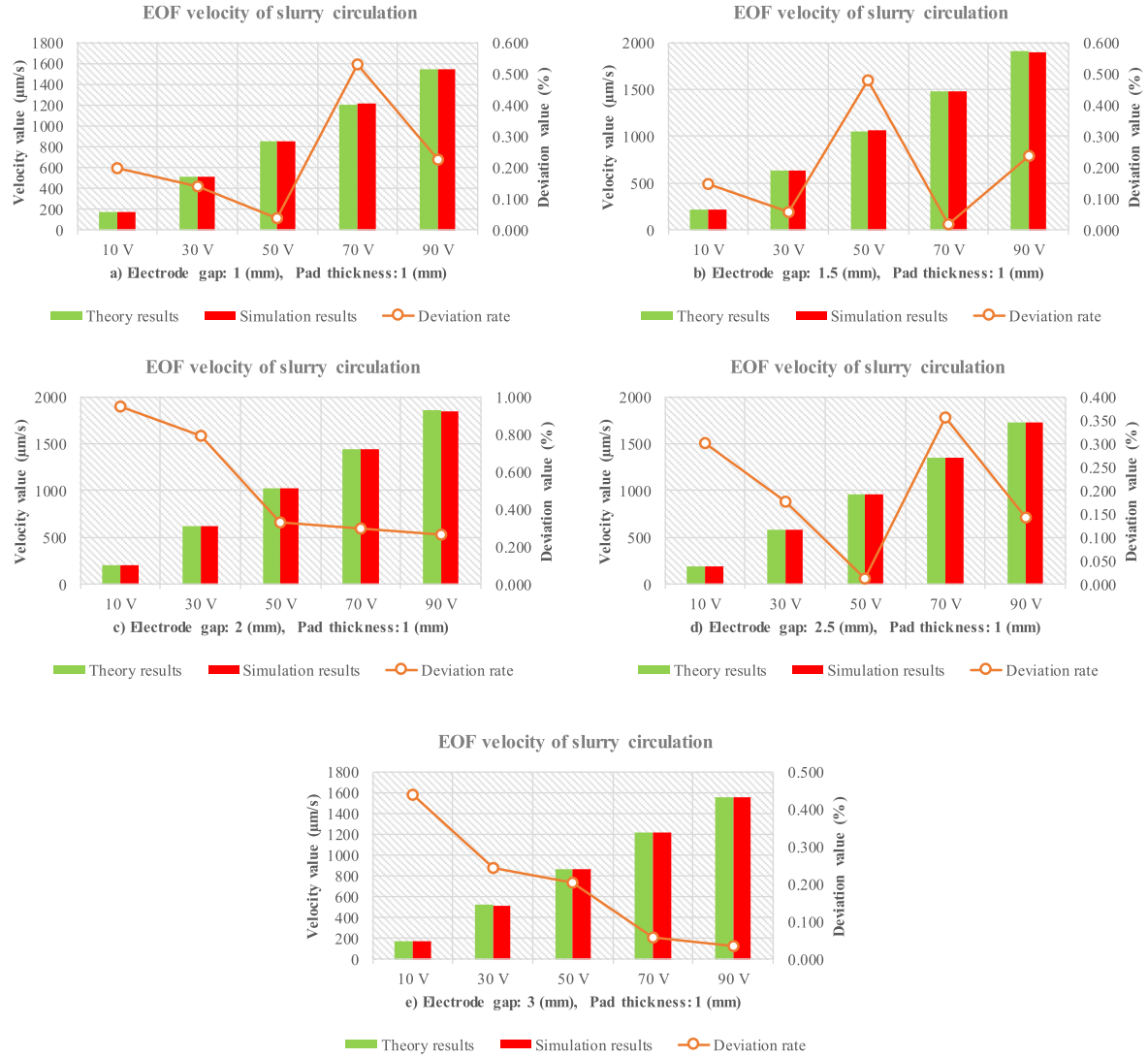
Figure 6. Comparison of the electro-osmosis flow velocity of slurry circulation between theoretical calculation and simulation results in the case of pad thickness of 1 mm, and various applied voltage levels such as 10V, 30V, 50V, 70V, 90V at different electrode gap (a) 1 mm, (b) 1.5 mm, (c) 2 mm, (d) 2.5 mm, (e) 3 mm.

was finally created with a high skewness of 0.61. Table I illustrates the simulation parameter in detail of the 3D-EOF cell model.

The integration of various physical modules of the COMSOL Multiphysics® software is applied, which mainly combines three different modules to define the 3D-EOF cell model including electric current module, laminar flow module, and particle tracing module. The current module is defined as the position of the positive and negative electrodes in the 3D-EOF cell model and the magnitude of the applied potential. Then result of electric field is added and generated by the current module to the laminar flow module. By selecting the boundary conditions for the EOF, the boundary conditions of the 3D-EOF cell model, the range, and direction of the flow velocity generated by the EOF in the entire liquid are mainly defined. The material condition of the flow module must be liquid, so the zeta potential of the polishing liquid is −0.1 V, and the relative dielectric constant is 80 for pure water. Finally, the analysis results of the laminar flow module are added to the particle tracing module. The overall dynamic simulation time is like the EKF-CMP process time of 500 s. According to the analysis result, the velocity component of each abrasive grain is obtained.

Based on the electric current module in COMSOL Multiphysics® software,[36] its electric field mainly uses the compositional relationship to describe the macroscopic characteristics of the medium. It

uses the electric displacement equation to define the electric displacement, the electric field, the material properties, and the relative permittivity

$$D = \varepsilon_0 \varepsilon_r E_t \qquad [8]$$

Where D is the electrical displacement, ε_0 is the relative dielectric constant, ε_r is the boundary constant, and Et is the electric field. However, in classical electromagnetism, when a dielectric is applied to an external electric field, due to the relative displacement of the positive and negative charges inside the dielectric, an electric dipole will be generated and electric polarization will occur. The applied electric field may be an external electric field. It may be the electric field generated by the free charge embedded in the dielectric, so the above equation can be rewritten as follow

$$D = \varepsilon_0 E_t + P_e \qquad [9]$$

where Pe = intensity of polarization.

Based on the laminar flow module in COMSOL Multiphysics® software, the Navier-Stokes equations are used as the calculation basis of the module.[36] In COMSOL, this system is assumed to be a control volume and mass conservation system. It describes the movement of collisions between molecules in the form of a pressure
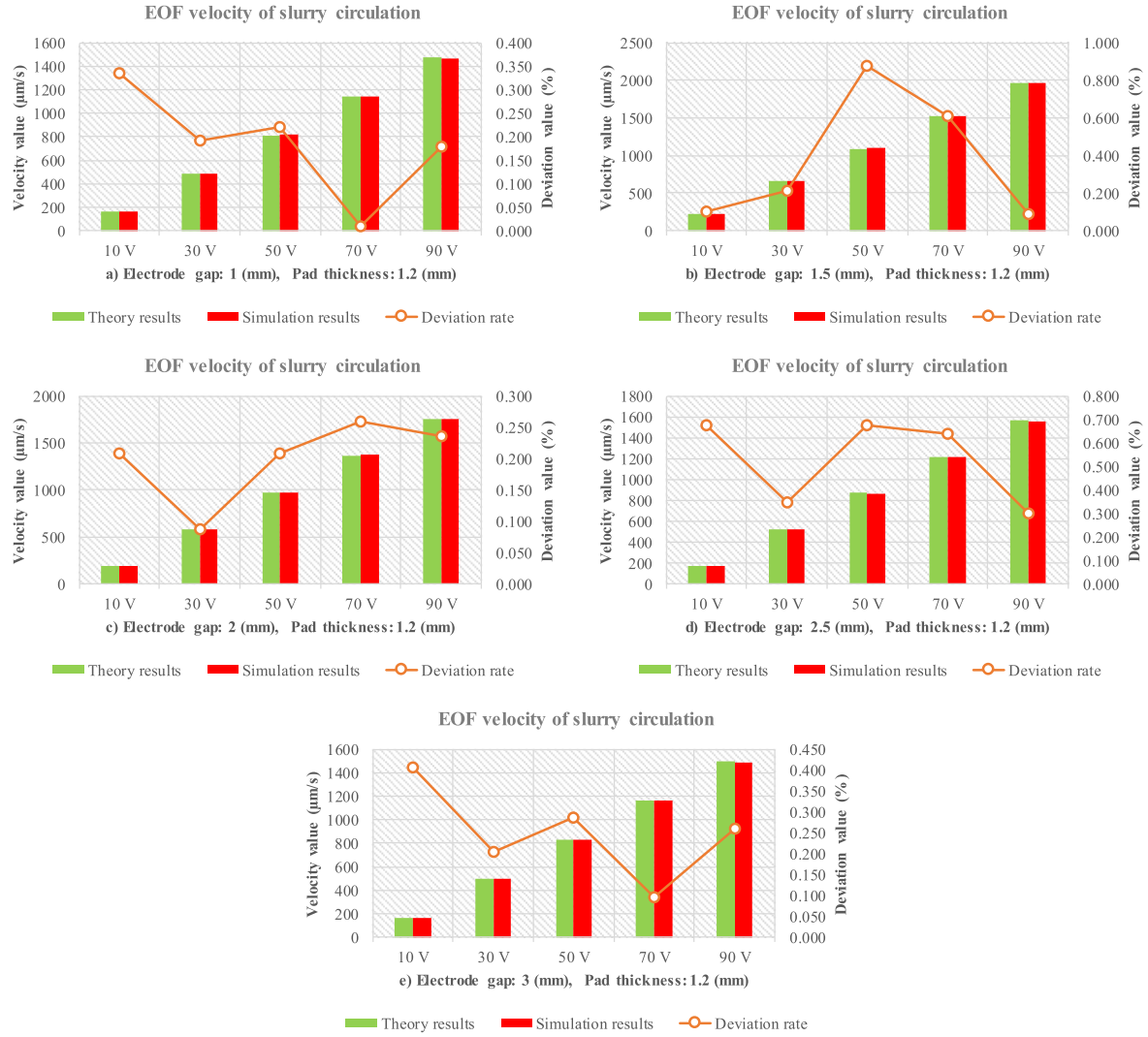
Figure 7. Comparison of the electro-osmosis flow velocity of slurry circulation between theoretical calculation and simulation results in the case of pad thickness of 1.2 mm and various applied voltage levels such as 10V, 30V, 50V, 70V, 90V at different electrode gap (a) 1 mm, (b) 1.5 mm, (c) 2 mm, (d) 2.5 mm, (e) 3 mm.

field. In a single-phase, the definition of single-phase flow liquid is an incompressible fluid and has constant density and viscosity under laminar flow conditions, which can be expressed by the Navier-Stoker equation

$$\rho\frac{\partial u}{\partial t} + \rho u.\nabla u = -\nabla p + \mu\nabla^2 u + \rho g + f_b \quad [10]$$

Where p is the fluid pressure, g is the acceleration due to the gravity, μ is the viscosity of the fluid, ∇^2 is the Laplacian operator, f_b is any other body force per unit volume, ρg is the body force, ρ is the fluid density, t is the time, ∇ is the scalar field, u is the fluid velocity. Because this module must be taken into account that the electric field in the current module generates an electric body force per unit fluid volume (f_{Et}), the EOF causes the abrasive particles to disturb the liquid, the electric field force can be rewritten as follow

$$f_{E_t} = \rho_f E_t \quad [11]$$

where ρ_f is the free charge density. The differential relationship between the electric field and the potential is as shown Eq. 12. Combining Eqs. 10 and 13, the final converted momentum equation is shown as Eq. 14

$$E_t = -\nabla\psi \quad [12]$$

$$f_E = -\rho_f\nabla\psi \quad [13]$$

$$\rho\frac{\partial u}{\partial t} + \rho u.\nabla u = -\nabla p + \mu\nabla^2 u + \rho g - \rho_f\nabla\psi \quad [14]$$

where $-\nabla\Psi$ is the electric potential,

The particle tracing method offers an attractive alternative to continuum-based numerical methods, such as the finite element method for modeling of species transport in strongly convicting flows. The particle tracing can be used to solve the abrasive particle motion. In the particle trajectories module in COMSOL Multiphysics® software which uses Newton's second law to solve the state of the particle position in the 3D-EOF cell model:[36]

$$\frac{d}{dt}(m_p v) = F_P \quad [15]$$

where t is the time, m_p is the particle mass, v is the particle velocity and Fp is the total force acting on the particle. However, the
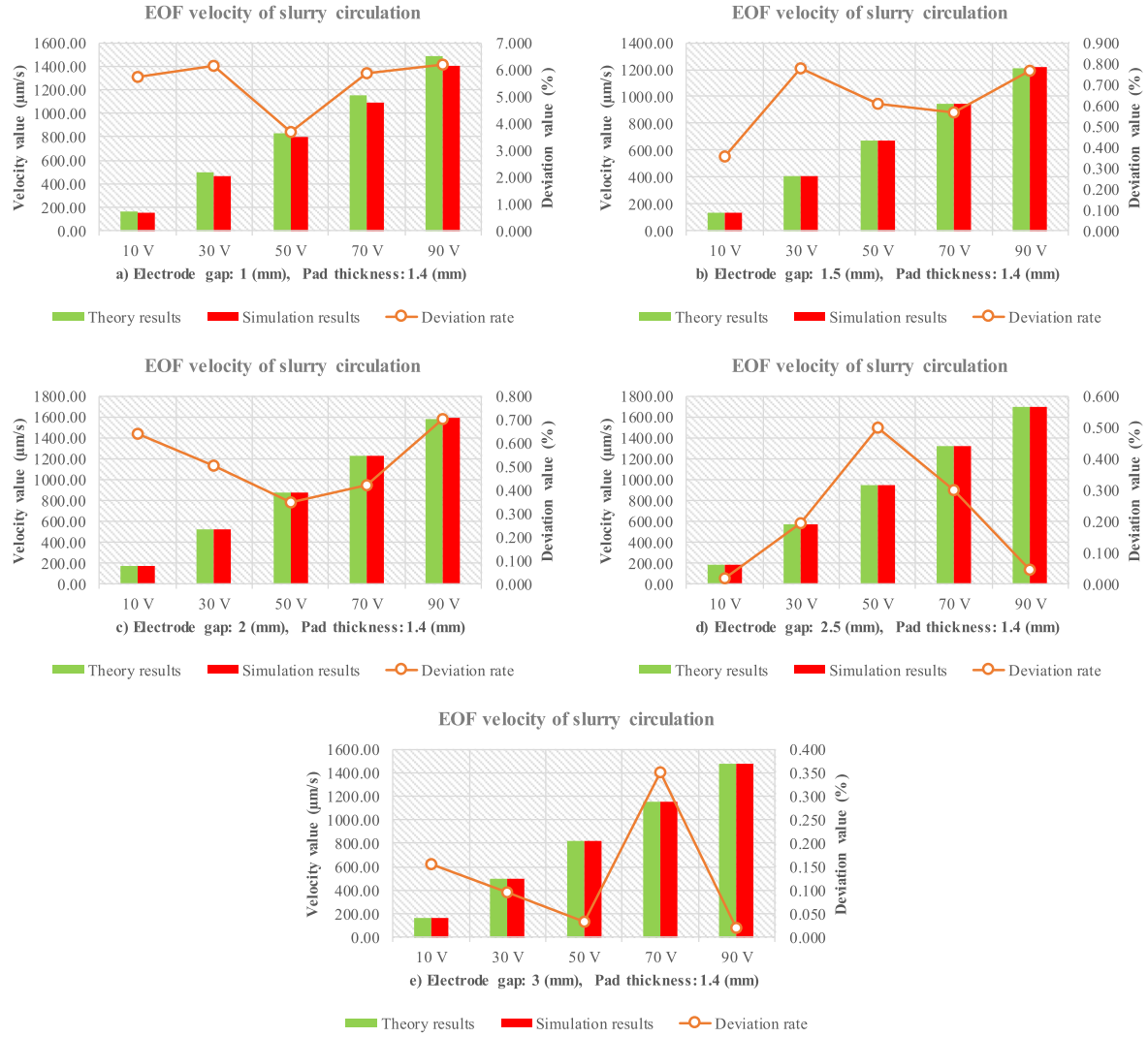
Figure 8. Comparison of the electro-osmosis flow velocity of slurry circulation between theoretical calculation and simulation results in the case of pad thickness of 1.4 mm, and various applied voltage levels such as 10V, 30V, 50V, 70V, 90V at different electrode gap (a) 1 mm, (b) 1.5 mm, (c) 2 mm, (d) 2.5 mm, (e) 3 mm.

perturbation of particles by EOF is derived from the force generated by the electric field, so the force of the electric field can be obtained by Coulomb's law as shown in Eq. 2. Under the combination of three different modules, the simulation results in the 3D-EOF cell model can be digitized to obtain the effect of each abrasive particle on the wafer.

Particle dynamics analysis in the 3D-EOF cell model.—Based on the particle trajectories simulation module in the COMSOL Multiphysics® software,[36] the motion of each particle in the 3D-EOF cell model is analyzed. Each of the particles is subjected to applied force from several different sources acting on it. These include gravitational and buoyancy force, stokes drag force, hydrodynamic pressure, electric force, and collision impulse forces that impose due to the motion of the fluid. The collision impulse force, drag force, and hydrodynamic pressure are applied in the three principal directions, while gravitational and buoyancy force is only applied in the z-direction and the electric force is applied in the x-direction.[37] The particle drag forces of the particle-free in the slurry film thickness of the 3D-EOF cell model is calculated as follow[36]

$$F_D = \frac{18\mu}{\rho_p d_p^2} m_p (u - v) \qquad [16]$$

where F_D is the particle drag force, d_P is the particle diameter, ρ_p is the particle density, μ is the fluid viscosity, m_p is the particle mass, u is the velocity of the fluid, v is the particle velocity.

The collision impulse force of the motion of the abrasive particles in the slurry of the 3D-EOF cell model is calculated as follows[38]

$$m_1 v_1 + m_2 v_2 = m_1 v_1' + m_2 v_2' \qquad [17]$$

$$\varepsilon = \frac{v_2' + v_1'}{v_1 - v_2} \qquad [18]$$

Where m_1 is the first particle mass, m_2 is the second particle mass, v_1 is the Pre-collision velocity of the first colliding particle, v_2 is the Pre-collision velocity of the second colliding particle, v_1' is the Post-collision velocity of the first colliding particle, v_2' is the Post-collision velocity of the second colliding particle, ε is the coefficient of restitution between two colliding objects.

The particle gravity force from the surrounding fluid is given as follow[36]

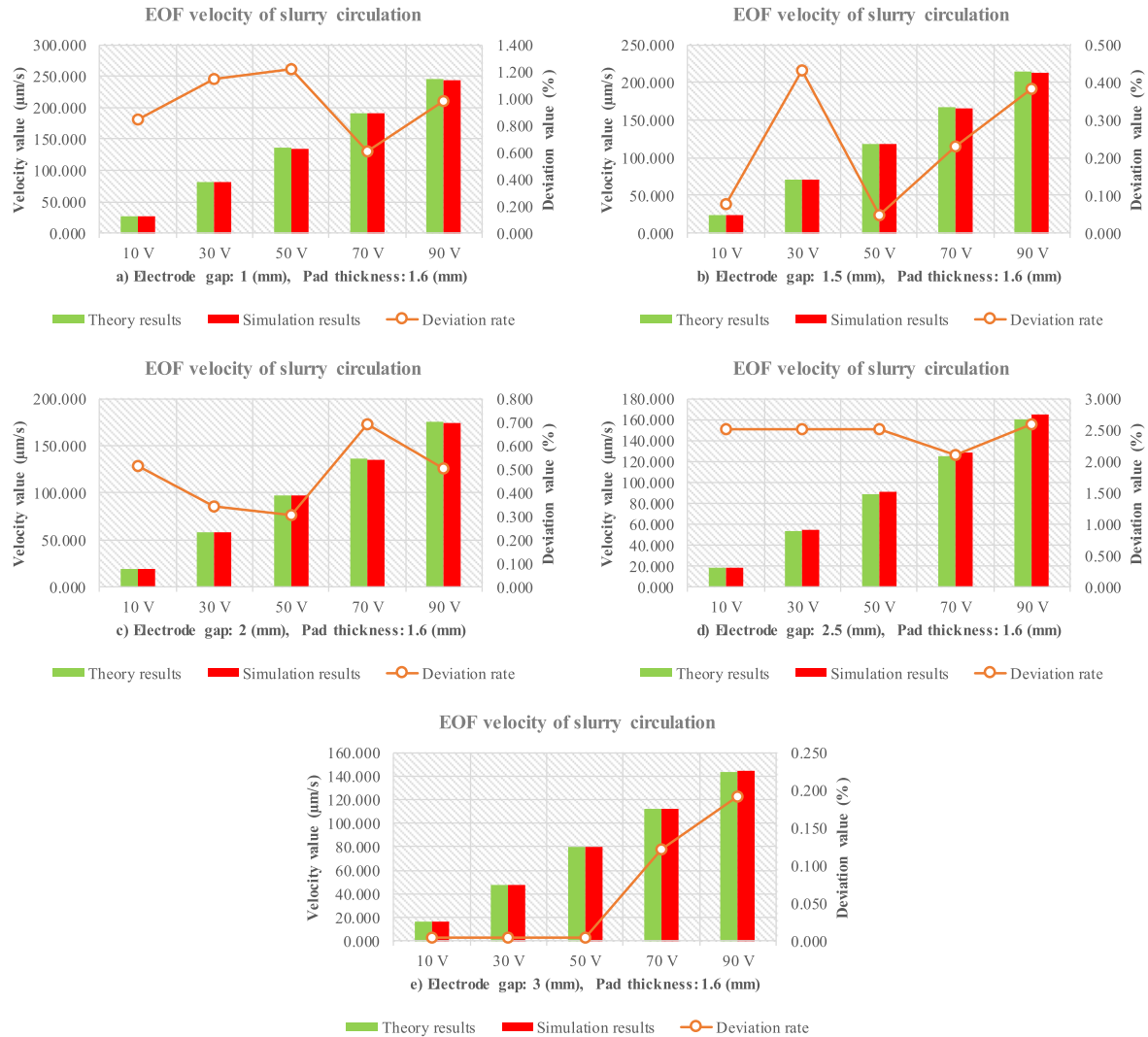$$F_g = m_p g \frac{\rho_p - \rho}{\rho_p} \qquad [19]$$

Figure 9. Comparison of the electro-osmosis flow velocity of slurry circulation between theoretical calculation and simulation results in the case of pad thickness of 1.6 mm, and various applied voltage levels such as 10V, 30V, 50V, 70V, 90V at different electrode gap (a) 1 mm, (b) 1.5 mm, (c) 2 mm, (d) 2.5 mm, (e) 3 mm.

Where g is the acceleration due to gravity, ρ_p is the particle density, ρ is the liquid density. This force acts only in the vertical direction. The 3D-EOF cell model is proposed based on some assumptions such as: the wafer is horizontal, the lubrication flow is a thin layer between the pad and the wafer surface, the pad, and the wafer surface are assumed flat and hard without surface roughness, the pad and wafer are impermeable, there is no-slip among the slurry and the pad and the wafer surface, the body forces are negligible at the quasi-steady state, the inertial and surface tension forces are negligible compared with viscous forces, the buoyancy force of abrasive particle is constant in all simulation. By applying the hydrodynamic lubrication theory in the 3D-EOF cell model, the slurry flow pressure is 1.5 psi through the lubricant film. The boundary condition of the normal stress is set to be zero. The wall-liquid interface is no-slip. The relative Reynolds number of particles in the fluid is small. The abrasive particles in the slurry are assumed as hard particle to maintain spherical shape with a given size distribution of the Gaussian distribution

Results and Discussion

One objective of this study is to investigate the number of the effective particle which is defined as the total number of the particle to contact with the wafer in the EKF-CMP system. The COMSOL Multiphysics® software is applied to build the 3D-EOF cell model for the simulation. The particle dynamic data at the various level in the slurry film thickness is shown during the simulation process. The simulation results are exported by the text file per second during the simulation time. The text file is analyzed by a code in the MATLAB software. The EKF-CMP system uses EOF to assist in driving the disturbance of the abrasive particles in the polishing liquid, and the grinding effect is achieved by the contact between the abrasive particles and the wafer surface. Therefore, the movement behavior of the abrasive particles has a great influence on the MRR of the wafer surface. The more active movement of the abrasive particles will create a higher frequency of the abrasive particles contacting the wafer surface, due to the greater material removal rate. Generally, the number of the effective particle is an index to consider the work effect of the polishing process. Its role is similar in particle dynamic theory, which is the fluctuation velocity of particles. The value of the EOF velocity of the slurry flow circulation is compared between the theoretical calculation results and simulation results by the 3D-EOF cell model.

Theoretical calculation results.—Based on the theory of the electro-osmosis flow as mentioned above, the 3D-EOF cell model is used to validate the correlation between the theoretical calculation results and the simulation results. In this study, the parallel staggered
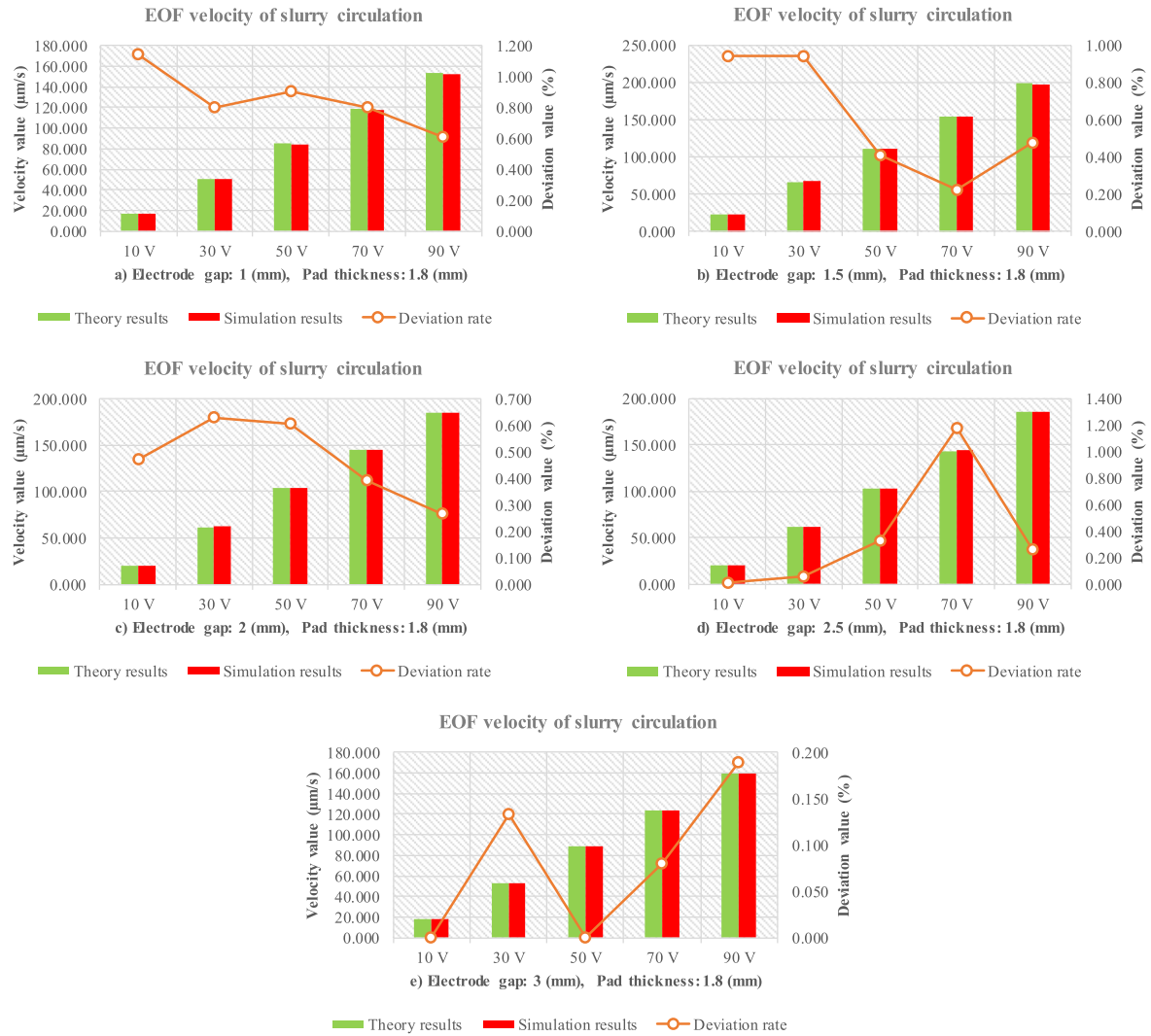
Figure 10. Comparison of the electro-osmosis flow velocity of slurry circulation between theoretical calculation and simulation results in the case of pad thickness of 1.8 mm, and various applied voltage levels such as 10V, 30V, 50V, 70V, 90V at different electrode gap (a) 1 mm, (b) 1.5 mm, (c) 2 mm, (d) 2.5 mm, (e) 3 mm.

electrodes of the coplanar cathode and anode are designed in the 3D-EOF cell model to create the tangential electrode of the concentric circle under the pad surface in the EKF-CMP system. The main purpose is to generate EOF through the tangential electrode design of the concentric circle to make the abrasive particles in the disturbed liquid to achieve a uniform benefit. The simulation results are shown in Fig. 5. The parallel staggered electrodes between positive and negative created more disorder of the abrasive particle motion due to the influence of the electrophoretic force from the positive electrode to the negative electrode of the electric field itself. The velocity of EOF is proportional to the magnitudes of the tangential electric field. From the analysis results of calculation and simulation data, it is known that the design of the parallel staggered electrodes between positive and negative can achieve higher flow field disturbances. The electro-osmosis mobility value is calculated as shown in Eq. 5 with the parameters such as the zeta potential is -0.1 V, the liquid dynamic viscosity is 0.001 kg/ m−s, the free space permittivity is 8.85×10^{-12} $C^2N^{-1}m^{-2}$, the relative permittivity is 80. According to the three-dimensional COMSOL simulation results, the maximum value of the tangential electric field intensity at the positive and negative electrodes in the 3D-EOF cell model are obtained in each case individually such as the electrode gap spacing, the direct current voltages, and the polishing pad thickness. For example, the value of the distributed strength of the

tangential electric field at the electro gap of 1 mm, the pad thickness of 2 mm, and the applied voltage of 50V is shown in Fig. 5b. The EOF velocity value of the slurry circulation is calculated by substitute the maximum tangential electric field value into Eq. 6. The calculation results are used as a basis to compare with simulation results. The total results of the calculation and simulation process in all of the cases are shown in Figs. 6–11. The deviation rate between calculation and simulation of the EOF velocity value of the slurry circulation in the 3D-EOF cell model is very small in each case individually. The deviation values are only 0.01–6%. Additionally, the parallel staggered electrodes between positive and negative have the optimal performance of the EOF rate in the abrasive particle dispersibility.

Simulation results.—In the analysis of the particle tracing simulation results, the total number of effective particles is used for the discussion. The simulation process of the 3D-EOF cell model has been conducted with different conditions such as the direct current voltages, the polishing pad thickness, and the electrode gap spacing. The simulation results are shown in Figs. 12 and 13. In all cases of the different pad thickness and the various electrode gap spacing, the total number of the wafer touch particles at steady-state tends to increase significantly with the applied bias voltage rises, because the applied energy of the electric field is strong which will
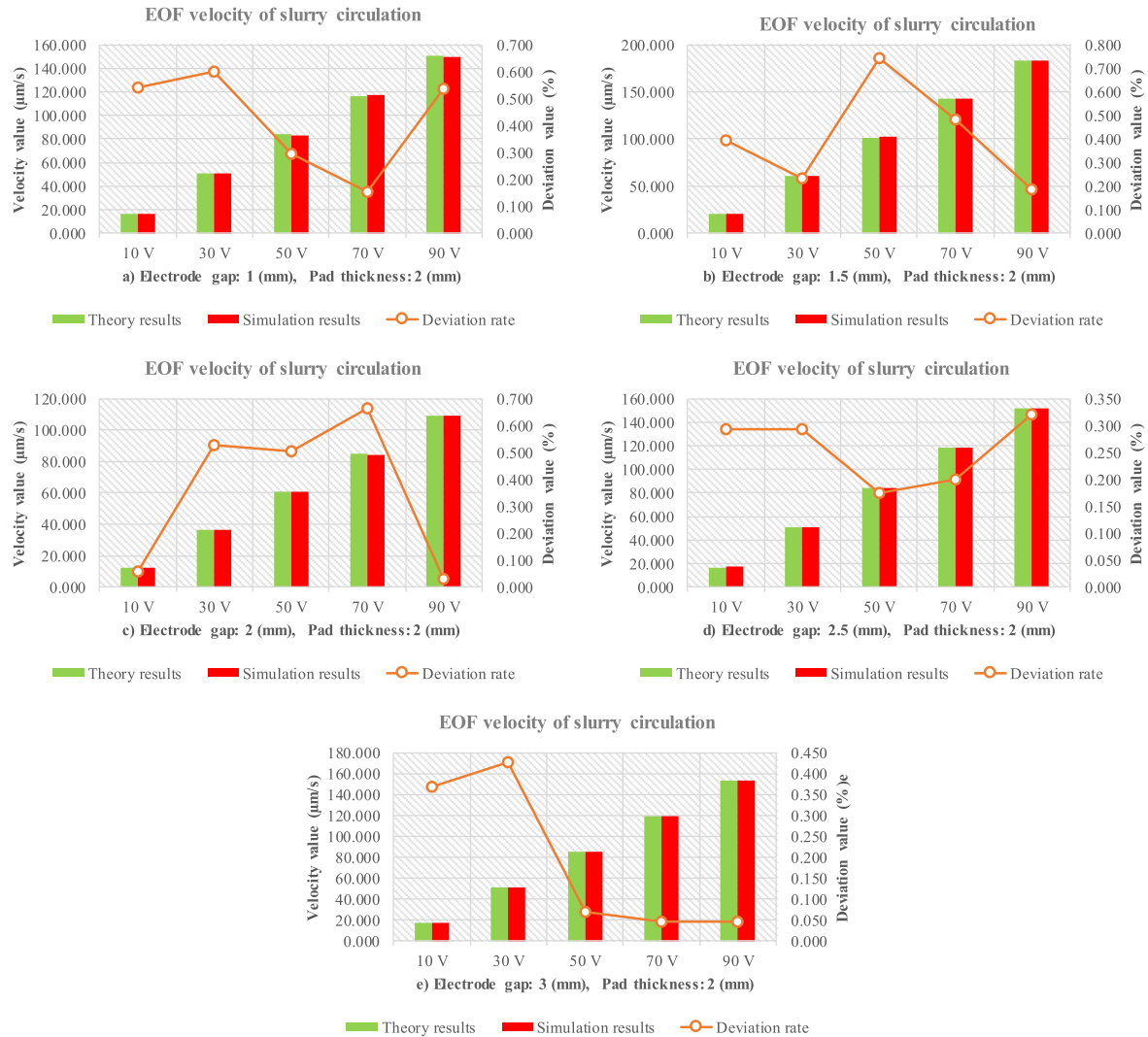
Figure 11. Comparison of the electro-osmosis flow velocity of slurry circulation between theoretical calculation and simulation results in the case of pad thickness of 2 mm, and various applied voltage levels such as 10V, 30V, 50V, 70V, 90V at different electrode gap (a) 1 mm, (b) 1.5 mm, (c) 2 mm, (d) 2.5 mm, (e) 3 mm.

fabricate the abrasive particle motion of the intense EOF disturbing. Especially, at the pad thickness of 1.2 mm, the electrode gap spacing such as 1 mm, 1.5 mm, 2 mm, 2.5 mm, 3 mm and the various applied voltage levels such as 10V, 30V, 50V, 70V, 90V are shown in Fig. 12b. The total number of effectual particles on the wafer at steady-state tends to decrease significantly according to the rules with the increasing electrode gap spacing which is compared based on the same of the voltage level. The total number of effective particles at steady-state is the biggest in the case of the electrode gap of 1 mm and is the smallest in the case of the electrode gap of 3 mm in all of the cases of the simulated voltage levels. This stability trend reduces according to the rules when electrode gap spacing increase from 1 mm to 3 mm which is also found from the simulation results in Fig. 12b. However, in all other cases of the electrode gap spacing increase from 1 mm to 3 mm as shown in Figs. 12a–12f and the pad thickness grows from 1 mm to 2 mm as shown in Figs. 13a–13e, the total number of effective particles at steady-state tends to decrease irregularly when it is compared based on the same voltage level.

On the other hand, the simulation designs of EOF at the different polishing pad thickness have been finished as a basic design in the EKF-CMP system. The primary purpose is to observe the changing of EOF strength by changing the polishing pad thickness with non-grooved and non-porosity to investigate the

total number of effective particles on the wafer at steady-state in each case individually. Figs. 12a–12f show the simulation results based on the various polishing pad thickness. The total number of effective particles on the wafer at steady-state tends to decrease with the increasing pad thickness from 1 mm to 2 mm, due to the PU polishing pad block hinders the electric field generated by the electrode. The higher pad thickness creates the weaker electric field strength and the weaker electro-osmosis flow. Therefore, the movement of the abrasive particles tends to significantly reduce. In addition, the total number of effective particles is the smallest in the case of the polishing pad thickness of 2 mm as shown in Figs. 13a–13e.

Additionally, the simulation designs of EOF at the various electrode gap spacing have been finished as a basic design in the EKF-CMP system. The main purpose is to observe the changing of the EOF strength by changing the electrode gap spacing to investigate the number of effective particles on the wafer at a steady-state in each case individually. Figs. 13a–13e show the simulation results based on the different electrode gap spacing. The total number of effective particles on the wafer at steady-state tends to reduce with the raising electrode gap from 1 mm to 3 mm since the adjustment of the electrode gap spacing will mainly change the influence range of the electric field. It is known from Coulomb's law that the generated electric field strength by the point charge is
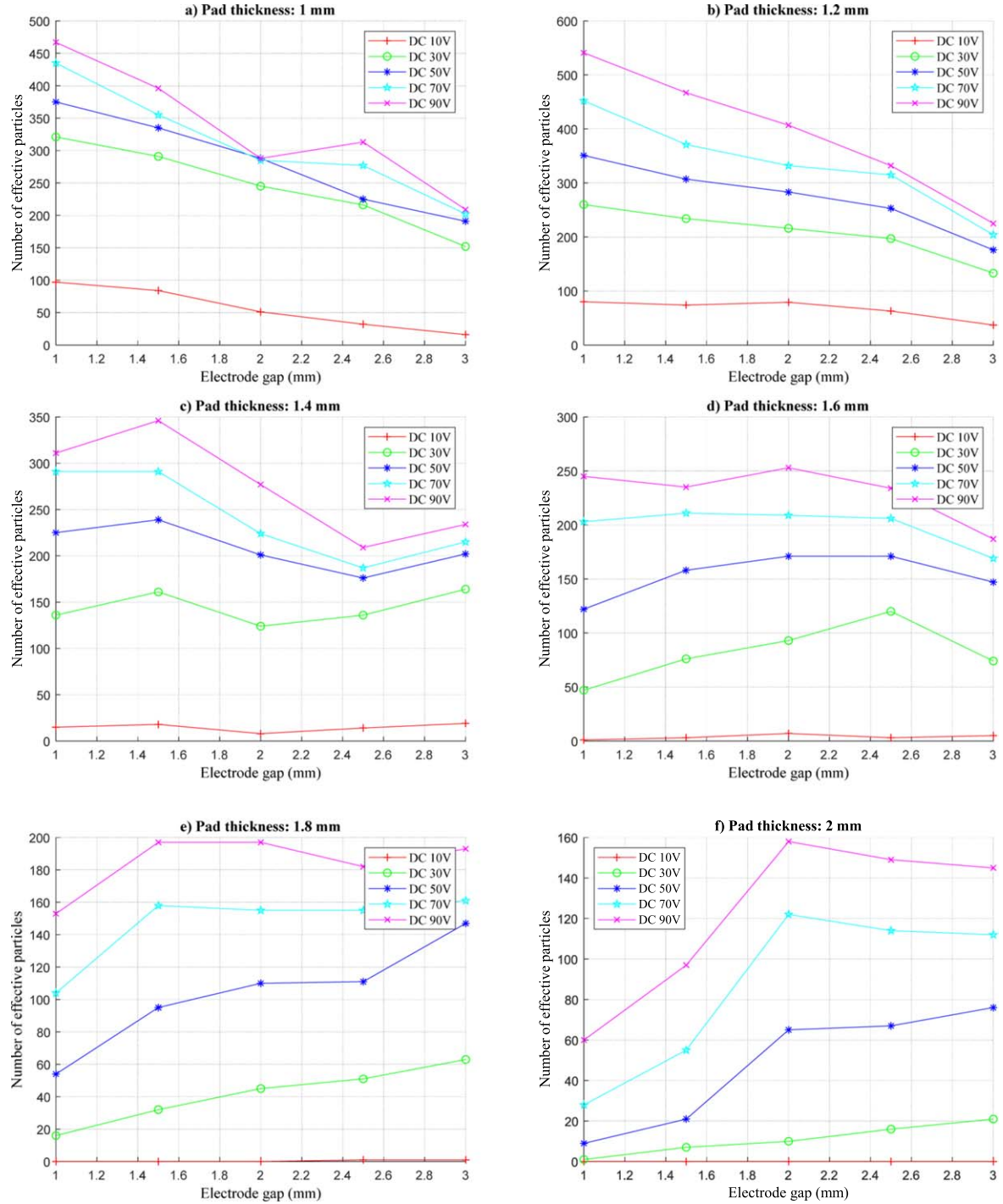
Figure 12. Relationship between different electrode gap spacing such as 1 mm, 1.5 mm, 2 mm, 2.5 mm, 3 mm and the total number of effective particles at various applied voltage levels such as 10V, 30V, 50V, 70V, 90V under various polishing pad thicknesses (a) 1 mm, (b) 1.2 mm, (c) 1.4 mm, (d) 1.6 mm, (e) 1.8 mm, (f) 2 mm.

proportional to the amount of the electricity it carried and is inversely proportional to the square of the distance. Therefore, the electrodes used in EKF-CMP must be taken into account the electric field density and the coverage of the entire wafer area. The farther electric field source is, the weaker electric field strength will be, and the weaker EOF leads to the number of the smaller effective particles as shown in Fig. 13e. The governing equation can be expressed in the form of Eq. 20 when the centrifugal and the electrostatic forces are balanced in the electrode gap spacing center[39]

$$m_p.\omega^3.r_c = n.e.E_t = \frac{n.e.V}{r_c \ln\left(\frac{r_2}{r_1}\right)} \qquad [20]$$

where m_p is the particle mass, ω is the rotation speed of the particle, r_c is the center of electrode gap, E_t is the electric field strength, V is the applied voltage, and r_1 and r_2 are the radii of the parallel
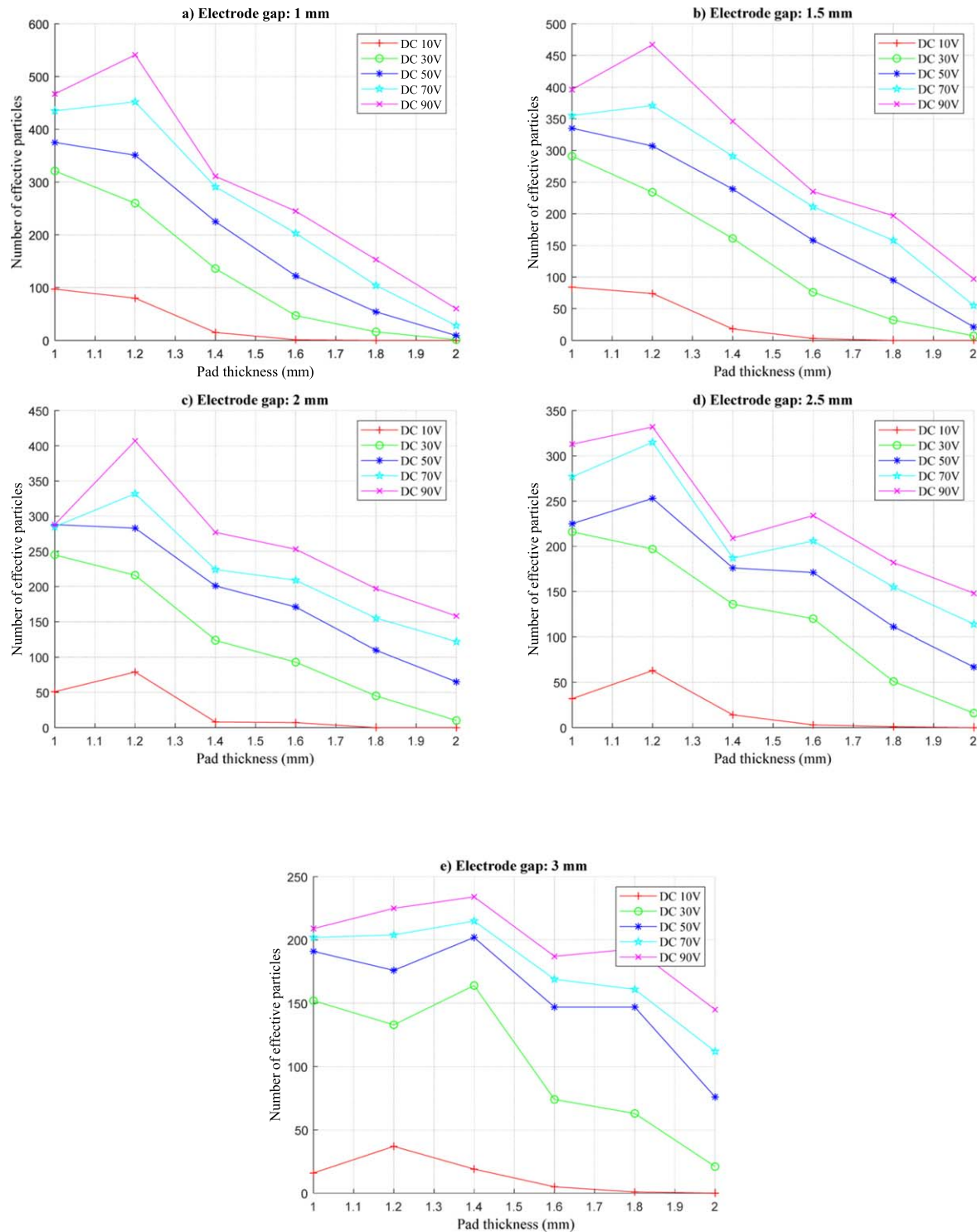
Figure 13. Relationship between various pad thickness such as 1 mm, 1.2 mm, 1.4 mm, 1.6 mm, 1.8 mm, 2 mm and the total number of effective particles at various applied voltage levels such as 10V, 30V, 50V, 70V, 90V under different electrode gap spacing (a) 1 mm, (b) 1.5 mm, (c) 2 mm, (d) 2.5 mm, (e) 3 mm.

staggered electrodes between positive and negative, respectively. n is the number of charges, e the elementary charge. Finally, the relationship between the total number of effectual particles and the various parameters such as the electrode gap spacing, the direct current voltages, the polishing pad thickness has been investigated. This research can be applied to chemical mechanical planarization and wafer polishing processes in the future as a benchmark for improving the EKF-CMP process.

Experimental results.—The objective of this experiment is to examine the effective work of the EKF-CMP process. The setup of the complete EKF-CMP system is shown in Fig. 14. The EKF-CMP system consists of a conductive ring, an electrode conductive plate, a power connection, and a power supply. In our research, the PM5 precision polishing machine of Logitech Co. Ltd. in the United Kingdom with the diameter of the polishing plate of 300 mm is used for the EKF-CMP process. The IC-1000 pad is chosen which has the
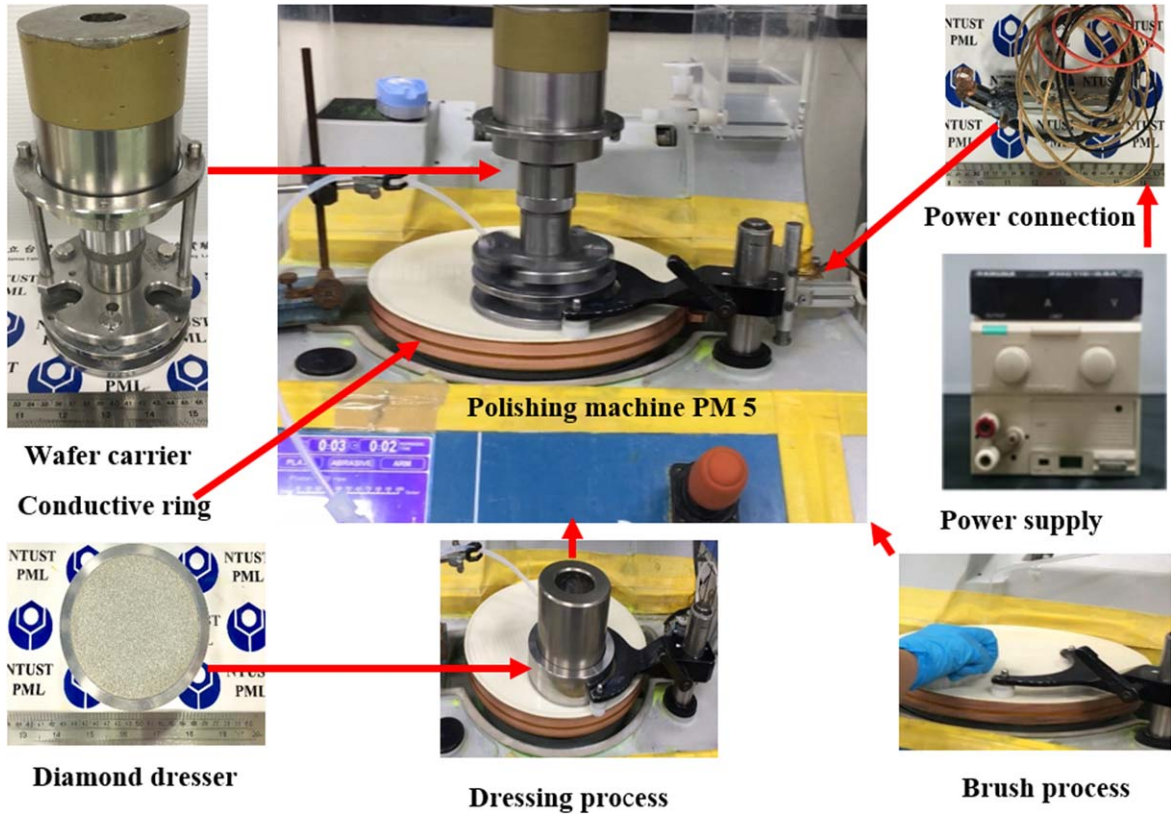
Figure 14. The EKF-CMP system.

Table II. EKF-CMP experimental parameter of blanket copper film wafer.

Parameters	Value (Unit)				
Polishing machine	PM5				
Pad type	IC-1000				
Groove width	0.5 mm				
Groove depth	0.36 mm				
Wafer type	Blanket copper film				
Wafer size	40 mm × 40 mm				
Applied pressure	1.5 psi				
Plate rotation speed	70 rpm				
Slurry type	Cabot C8902				
SiO_2 concentration	0.3 wt%				
Abrasive size	34 nm				
H_2O_2 addition	0.45 wt%				
PH value	3–4				
Slurry flow rate	50 (ml/min)				
Dressing time	1 min				
Brush time	1 min				
Polishing time	3 min				
DC voltage application	0V	10V	30V	50V	70V	90V

detailed dimensions of the pad groove as shown in Table II. The pad is carefully cleaned before and after every single experiment by the dressing and brush process with DI-Water. The blanket copper film wafer is attached to the wafer carrier, and the applied wafer size of this machine is 40 mm × 40 mm. Additionally, the polishing liquid is the commercial C8902 slurry for copper film wafer in CMP and EKF-CMP experiment. The basic physical properties of the C8902 slurry are as follows, the abrasive type in C8902 is Colloidal Silica, the abrasive size is 34 nm, the SiO_2 concentration is 0.3 wt%, the
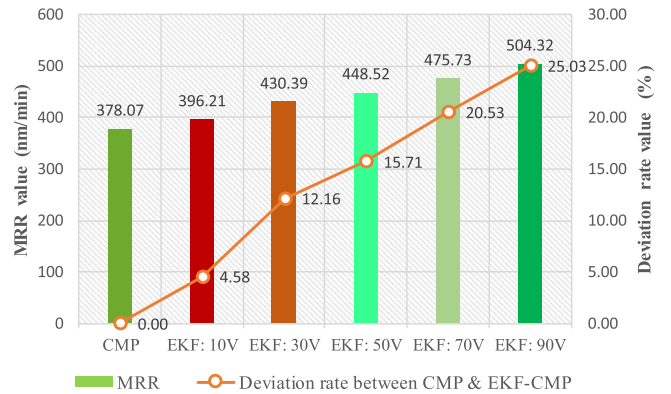

Figure 15. The experimental results of the MRR variation of the CMP and EKF-CMP process.

H_2O_2 addition is 0.45 wt%. According to the actual measurement results of the C8902 slurry by the Brookfield Viscometer DV-II + Pro tool in our Lab, the average pH value of the C8902 slurry is about 3.5 corresponding to the zeta potential is −0.1 V at the temperature of 30 degrees. The experiment conditions of the polishing process are set up as follow: the applied load block on the wafer carrier is 1.5 Psi, the pad rotation speed is 70 rpm. The polishing time is three minutes and the dressing and brush time is 1 min for each process. The slurry flow rate is 50 ml/min. The series of the polishing experiments are carried out at different voltages such as 10V, 30V, 50V, 70V, and 90V to compare the performance between the CMP and EKF-CMP process. The change parameters of the wafer surface such as material removal rate (MRR), non-uniformity (NU), and the surface roughness of the wafer surface after the CMP and EKF CMP process are investigated.

In this research, the material removal rate is estimated by the measurements of the weight variation of the wafer before and after
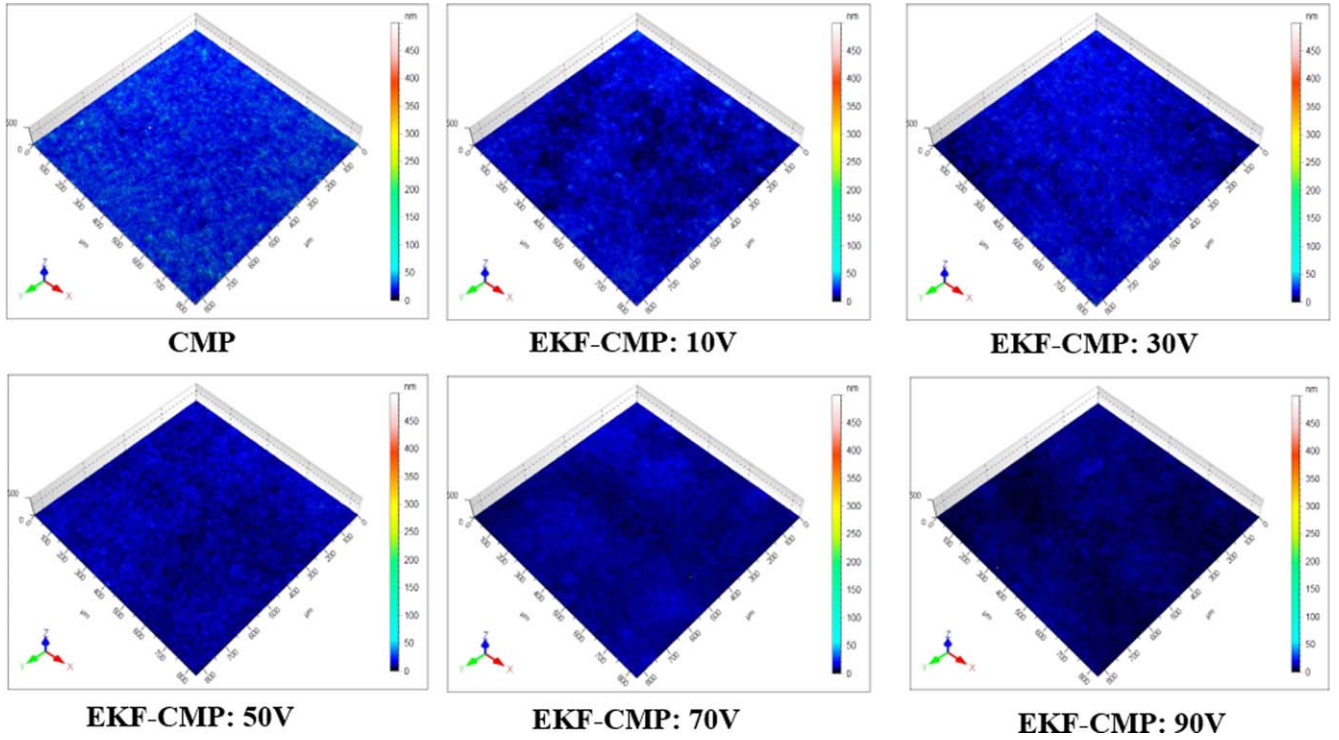
Figure 16. Comparison results between the CMP and EKF-CMP process of surface morphology under the different voltages.
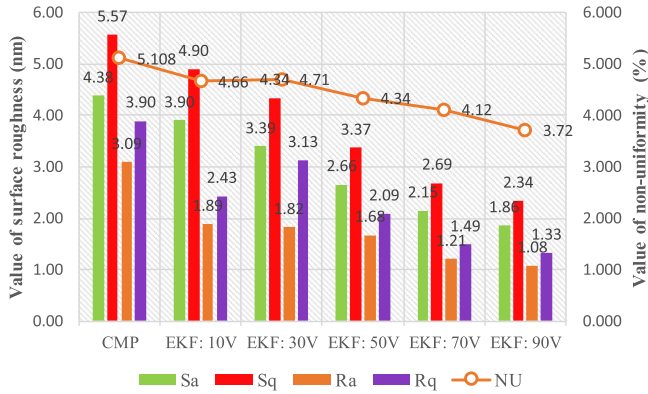

Figure 17. The comparison results of the surface roughness and non-uniformity of the wafer between the CMP and EKF-CMP process.

the CMP and EKF-CMP process. The weight value is measured by Mettler Toledo AlThe-204 and the MRR can be calculated as follow

$$MRR = \frac{\Delta W}{\rho \times A \times t}\left(\frac{nm}{min}\right) \qquad [21]$$

where ΔW is the variation of the wafer weight change (g), ρ is the wafer material density (g/cm^3), A is the wafer area (mm^2), t is the CMP process time (min). The experimental measurement results of the MRR variation are shown in Fig. 15. In the conditions of the different voltages of 0V (CMP), 10V, 30V, 50V 70V, and 90V, the material removal rates are 378.07, 396.21, 430.39, 448.52, 475.73, and 504.32 nm/min, respectively. The deviation rate between the CMP and EKF-CMP process at the different voltages are 4.58%, 12.16%, 15.71%, 20.53%, 25.03%, respectively. The best MRR improvement rate is 25.03% at the voltage of 90V. Additionally, the change variation of the copper film thickness is measured by Quatek QT-50 tool at the five-point probe of the copper film thickness which can be used as the evaluation of non-uniformity (NU). The value of the thickness variation is calculated as follow

$$NU = \frac{Thickness\,(max) - Thickness\,(min)}{Thickness\,(average)} \times 100\% \qquad [22]$$

The surface morphology of each case is shown in Fig. 16. The surface roughness tends to be flat when the voltages increase. The surface roughness values and the non-uniformity are shown in Fig. 17. The surface roughness values are measured by Talysurf CCI lite system. The values of Sa, Sq, Ra, Rq of the CMP process 0V are 4.38 nm, 5.87 nm, 3.092 nm, 3.098 nm, respectively. The values of Sa, Sq, Ra, Rq of the EKF-CMP process at 90V are 1.86 nm, 2.34 nm, 1.08 nm, and 1.33 nm, respectively. From the analysis results of the three-dimensional surface roughness Sa decreased from 4.38 nm to 1.33 nm. The surface non-uniformity value has a significant downward trend at the increasing voltage and NU has decreased from 5.108% to 3.72%. Finally, based on the experimental results, it is known that the EKF-CMP process is superior to the traditional CMP process in terms of material removal rate, wafer non-uniformity, and surface roughness because the electric field strength promotes the uniform spread of the abrasive particles on the polishing pad which can improve the quality of ultra-flat surface with high efficiency.

Conclusions

This study has been developed and simulated a 3D-EOF cell model by COMSOL Multiphysics® software to investigate the total number of effective particles on the wafer in the EKF-CMP system. The simulation results estimated the total number of effective abrasive particles on the wafer surface. The electro-osmosis flow velocity value of the slurry flow circulation was similarly obtained between the theoretical calculation and simulation results under the various simulation conditions such as the electrode gap spacing, the direct current voltage levels, and the polishing pad thickness. The total number of effective abrasive particles on the wafer at steady-state of the simulation process increases dramatically with the intensifying electrode voltage and reduces significantly with as increasing electrode gap and raising pad thickness. The experimental results show that the EKF-CMP system at the 90V can improve

MRR with 25.03%, wafer surface roughness Sa with 2.52 nm, and non-uniformity of 1.39% as compared with the original CMP process. This result provides a deeper understanding of the important role of the assistance of electro-kinetic force during the CMP process. Furthermore, it can be used to analyze the abrasive particle action on the pad polishing surface affecting the surface polishing qualification of a wafer to achieve ultra-smooth surface with high efficiency.

ORCID

Phuoc-Trai Mai ⓘ https://orcid.org/0000-0002-8770-6545

References

1. C. C. A. Chen, L. S. Shu, and S. R. Lee, *J. Mater. Process. Technol.*, **140**, 373 (2003).
2. C. C. A. Chen and Q. P. Pham, *Int. J. Adv. Manuf. Technol.*, **91**, 3573 (2017).
3. H. Hocheng and Y. L. Huang, *Int. J. Mater. Prod. Technol.*, **18**, 469 (2003).
4. P. B. Zantye, A. Kumar, and A. K. Sikder, *Mater. Sci. Eng. R-Rep.*, **45**, 89 (2004).
5. R. K. Pal, R. Sharma, P. K. Baghel, H. Garg, and V. Karar, *J. Mech. Sci. Technol.*, **32**, 3835 (2018).
6. Q. Xu, L. Chen, J. Liu, and H. Cao, *ECS J. Solid State Sci. Technol.*, **8**, P370 (2019).
7. Q. Xu, L. Chen, and H. Cao, *ECS J. Solid State Sci. Technol.*, **8**, P821 (2019).
8. Q. Xu, L. Chen, J. Liu, and H. Cao, *ECS J. Solid State Sci. Technol.*, **9**, 074002 (2019).
9. C. C. Wei, J. H. Horng, A. C. Lee, and J. F. Lin, *Wear*, **270**, 172 (2011).
10. M. Uneda, K. Takano, K. Koyama, H. Aida, and K. I. Ishikawa, *Mech. Eng. J.*, **3**, 15 (2016).
11. T. L. Horng, *Int. J. Adv. Manuf. Technol.*, **37**, 323 (2008).
12. R. Han, Y. Sampurno, S. Theng, F. Sudargho, Y. Zhuang, and A. Philipossian, *ECS J. Solid State Sci. Technol.*, **6**, P32 (2017).
13. C. C. A. Chen, P. T. Mai, and W. H. Tien, *International conference on planarization/CMP technology* (2019).
14. J. C. Mariscal, Y. Sampurno, D. Slutz, and A. Philipossian, *ECS J. Solid State Sci. Technol.*, **9**, 024005 (2020).
15. Y. B. Tian, S. T. lai, and Z. W. Zhong, *Adv. Mater. Res.*, **565**, 324 (2012).
16. J. C. Mariscal, J. Mcallister, Y. Sampurno, J. S. Suarez, M. O'Neill, H. Zhou, M. Grief, and A. Philipossian, *ECS J. Solid State Sci. Technol.*, **9**, 044008 (2020).
17. C. Myant, M. Fowell, H. A. Spikes, and J. R. Stokes, *Tribol. Trans.*, **53**, 684 (2010).
18. P. Zhou, D. Guo, R. Kang, and Z. Jin, *Int. J. Adv. Manuf. Technol.*, **69**, 1009 (2013).
19. J. V. Kumar and R. R. Rao, *Tribol. Ind.*, **37**, 161 (2015).
20. Y. Huang, D. Guo, X. Lu, and J. Luo, *Microelectron. Eng.*, **88**, 2862 (2011).
21. D. G. Thakurta, C. L. Borst, D. W. Schwendeman, R. J. Gutmann, and W. N. Gill, *J. Electrochem. Soc.*, **148**, 207 (2001).
22. N. Y. Nguyen, Y. Tian, and Z. W. Zhong, *Int. J. Adv. Manuf. Technol.*, **75**, 97 (2014).
23. Z. Qi, W. Lu, and W. Lee, *Int. J. Mach. Tools Manuf*, **82–83**, 59 (2014).
24. Q. Mai, Y. Quan, P. Liu, and G. Ding, *Int. J. Adv. Manuf. Technol.*, **91**, 3493 (2017).
25. K. S. Chen, H. M. Yeh, J. L. Yan, and Y. T. Chen, *Int. J. Adv. Manuf. Technol.*, **42**, 1118 (2009).
26. F. Y. Lou, *Appl. Mech. Mater.*, **44–47**, P1213 (2011).
27. Y. Yoon, M. Baig, and D. Lee, *J. Korean Phys. Soc.*, **53**, 2129 (2008).
28. B. Egan and H. J. Kim, *ECS J. Solid State Sci. Technol.*, **8**, P3206 (2019).
29. Y. H. Tsai1 and C. C. A. Chen, *IEEE 2016 China Semiconductor Technology International Conference* (2016).
30. L. S. Lu, Y. M. Lin, and C. C. A. Chen, *IEEE 2018 International Conference on Advanced Manufacturing* (2018).
31. L. S. Lu and S. S. Hsiau, *Powder Technol.*, **184**, 31 (2003).
32. L. S. Lu and S. S. Hsiau, *Powder Technol.*, **184**, 31 (2008).
33. B. Potocek, B. Gas, E. Kenndler, and M. Stedry, *J. Chromatogr. A*, **709**, 511 (1995).
34. Z. Y. Xie and Y. J. Jian, *Colloid Surf. A-Physicochem. Eng. Asp.*, **461**, 231 (2014).
35. L. M. Fu, J. Y. Lin, and R. J. Yang, *J. Colloid Interface Sci.*, **258**, 266 (2003).
36. R. W. Pryor, *Multiphysics Modeling Using COMSOL* (JONES AND BARTLETT PUBLISHERS, U.S.A) (2011).
37. K. Yoshida, T. Sato, S. I. Eom, J. W. Kim, and S. Yokota, *Sens Actuators A Phys.*, **265**, 152 (2017).
38. E. J. TerreII and C. F. Higgs III, *J. Tribol. -Trans.*, **129**(4)933 (2007).
39. S. Kimotoa, W. D. Dickb, B. Huntb, W. W. Szymanskic, P. H. McMurrya, D. L. Robertsb, and D. Y. H. Pui, *Aerosol Sci. Technol.*, **51**(8), 936 (2017).